JOURNAL OF SOLID STATE CHEMISTRY 86, 195–205 (1990)

Stability, Structure Refinement, and Magnetic Properties of β-$Fe_2(PO_4)O$

M. IJJAALI, B. MALAMAN, AND C. GLEITZER

Laboratoire de Chimie du Solide Minéral, UA, 158, Université de Nancy I, BP 239, 54506 Vandoeuvre-les-Nancy Cedex, France

AND J. K. WARNER, J. A. HRILJAC, AND A. K. CHEETHAM

Chemical Crystallography Laboratory, Oxford University, 9 Parks Road, Oxford OX1 3PD, United Kingdom

Received November 17, 1989

We previously reported the existence and properties of a low-temperature modification of metastable β-$Fe_2(PO_4)O$. Its structure was proposed by analogy with $NiCr(PO_4)O$, but the magnetic measurements were hampered by traces of Fe_3O_4. We have now obtained a purer sample and a single crystal, allowing precise structure refinement, detailed magnetic characterization, and an investigation of the temperature stability range. The single crystal X-ray study confirms the structure as previously proposed: tetragonal ($Z = 4$), SG $I4_1/amd$, with a single iron site in face-sharing octahedra, and isolated PO_4 tetrahedra; the reliability factor is $R = 0.0345$ ($R_w = 0.0363$). The magnetic susceptibility has been measured from 4 to 850 K. The magnetization at zero applied field is around 0.01 emu/g at 300 and 88 K, and 0.04 emu/g at 3.5 K. The $\chi = f(T)$ curve displays several unusual features: above T_N (408 K) the Curie constant continuously decreases as a consequence of short-range magnetic order; below 100 K the susceptibility displays a small second maximum at 12 K. The magnetic structure has been investigated by low temperature powder neutron diffraction methods. At 17 K the Fe (II/III) spins are ordered ferromagnetically within the chains of face-sharing FeO_6 octahedra, with the spin direction along (001). The chains are ordered antiferromagnetically with respect to each other. The phase stability has been investigated by high temperature X-ray diffraction. The nonreversible $\beta \rightarrow \alpha$ transition takes place at ~800°C and is completed at ~840°C; however, the β phase stability is slightly lower in the presence of $FeCl_2$ traces or under high pressure.

Introduction

We have recently pointed out the existence of a low-temperature modification of the mixed-valence iron oxyphosphate, $Fe_2(PO_4)O$, which we have called β because it is metastable and transforms in an irreversible way into α-$Fe_2(PO_4)O$ (1). In the above publication, we have proposed the detailed structure as built from rows of FeO_6 face-sharing octahedra, running along the [100] and [010] directions of the tetragonal cell. The orthogonal rows share a common corner of the octahedra. The PO_4 tetrahedra are isolated. However, the above structure is based on the similarity between the X-ray powder diffraction patterns of β-$Fe_2(PO_4)O$ and $NiCr(PO_4)O$, the structure of which we established from a single-crystal analysis. But, in spite of the satisfactory reliability index ($R = 0.07$) obtained in the powder refinement, some uncertainties re-

0022-4596/90 $3.00

main as regards the true space group and the precise interatomic distances and angles.

In addition, the magnetic properties of β-$Fe_2(PO_4)O$ have only been outlined in the preceding publication: the temperature range of the susceptibility measurements was limited to the 100–700 K range and the observations were somewhat perturbed by traces of magnetite. It seemed therefore desirable to widen the measurement range and to work with purer samples.

We want to stress that any progress regarding β-$Fe_2(PO_4)O$ is valuable because this compound is of substantial interest. As far as we know (*2*), this is the first mixed-valence iron compound with a mean oxidation number 2.5, a single crystallographic site, and face-sharing octahedra. Therefore the situation is ideal for theoretical treatments, particularly as the extremely short iron–iron distance raises the question of competition between electron transfer due to the large *d*-orbital overlap and electron crystallization due to high electrostatic repulsion. Accordingly we have made additional efforts in order to obtain single-crystal structural data and magnetic measurements on a purer sample. We have also undertaken a determination of the magnetic structure by powder neutron diffraction. In a further publication we will discuss the electron transfer in detail as a result of further Mössbauer investigations.

Preparation, Crystallization, and Stability

The preparation has been described in our previous publication (*1*); however, some modifications have been introduced in order to obtain a more crystalline and monophasic product:

(i) The initial solution is now made from H_3PO_4 (rather than $(NH_4)_2HPO_4$), in order to avoid any hydrolysis of $Fe(NO_3)_3$.

(ii) The product obtained at 450°C in H_2–H_2O is sealed in a silica tube, with ~2% (weight) $FeCl_2$, and annealed at 600°C for one month. It then contains small crystals (size ~20 μm) in clusters; these are treated with ultrasound, yielding some isolated crystals, one of which could be transferred to the diffractometer holder.

It is worth noting that the following crystallization methods failed:

(i) Chemical vapor transport, with $FeCl_2$ or HCl, in a gradient always produced crystals of α-$Fe_2(PO_4)O$ or Fe_3O_4, probably because β-$Fe_2(PO_4)O$ is metastable.

(ii) Hydrothermal treatment at 600°C, 4 kbars, produced a hydrolysis of $Fe_2(PO_4)O$ into $H_3PO_4 + Fe_3(PO_4)_2 + Fe_2O_3$.

(iii) High pressure (50 kbars) annealing at 600°C gave a dense but polycrystalline product.

This is linked to the fact that β-$Fe_2(PO_4)O$ has a limited stability and transforms into α-$Fe_2(PO_4)O$ in an irreversible way. To obtain more information about that transformation, a sample has been slowly heated, under vacuum, within an X-ray diffractometer, with $\Delta T/\Delta t = 20$ K/hr. The patterns have been recorded in the range $\theta = 9$ to 12° (Co$K\alpha$ radiation), each scan lasting around 15 min. Within this diffraction range, we have the following lines:

	(*hkl*)	*d*(Å)	θ(°)	I/I_{max}
β-$Fe_2(PO_4)O$	(101)	4.91	10.5	26
α-$Fe_2(PO_4)O$	(101)	5.25	9.81	22
	(011)	4.88	10.56	20

Accordingly, the (101)β and (011)α are superposed and the $\beta \rightarrow \alpha$ transformation will mainly consist of the appearance of the (101)α line, although some intensity change may be observed at 10.50–10.56° (because I_{max} is not necessarily the same in both phases).

The results, shown in Fig. 1a, clearly indicate that the transformation starts at around 800°C and is finished at around 840°C. After cooling to room temperature, we find that no reverse transformation has

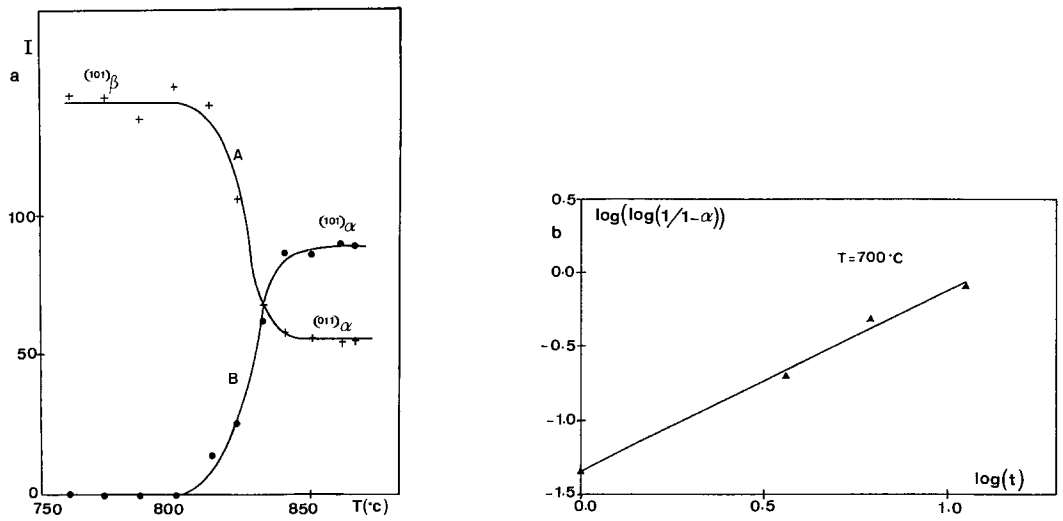

FIG. 1. (a) Intensity of X-ray diffraction lines vs temperature for α- and β-$Fe_2(PO_4)O$. (b) α, transformed fraction; t, time in days.

occurred. However, the following observations are worth mentioning:

(i) The presence of a small amount of $FeCl_2$ (1% weight) favors the $\beta \rightarrow \alpha$ transformation: for instance, annealing for 90 min at 750°C retains the β modification when pure, but totally converts it into α when $FeCl_2$ is present.

(ii) High pressure slightly favors the $\beta \rightarrow \alpha$ transformation, in spite of the fact that the densities are very close: 4.18 for α and 4.17 for β. Indeed, 15 min annealing at 750°C with 50 kbars (5 GPa) transforms β into α.

At 700°C, the transformation is slow enough to be recorded along several days. The transformed fraction α has been measured by X-ray diffraction for times ranging from 1 day to 11 days, and the $\log(\log(1/1 - \alpha))$ has been plotted versus $\log t$ in Fig. 1b. The slope of the line is 1.2 (correlation coefficient 0.99), which according to Rao and Rao (12) indicates that nucleation takes place at the beginning of the transformation. The rate constant, defined by

$$\alpha = 1 - \exp(-kt^n),$$

may also be calculated; we find $k = 0.15$ and $n = 1.2$.

Structure Refinement

A nearly spherical single crystal (diameter ~20 μm) was mounted on a NONIUS CAD 4 diffractometer. The cell parameters were determined by least-squares refinement of the 2θ values of 25 independent reflections, measured on the diffractometer. The structure refined satisfactorily in space group $I4_1/amd$ ($R = 0.034$) with the atomic positions of $NiCrPO_5$ (1) used as the starting point. Absorption has been neglected ($\bar{\mu}r \approx 0.15$). The conditions for the collection of the single crystal data and the refinement of the structure are listed in Table I. The scattering factors (Fe^{2+}, Fe^{3+}, P^0, and O^{-1}) and f' and f'' were taken from Ref. (*3*). All computer programs used were taken from Ref. (*4*). A list of the structure factors can be obtained from the authors on request.

The final positions and thermal parameters are listed in Table II, and the inter-

TABLE I

SUMMARY OF DATA COLLECTION AND STRUCTURE REFINEMENT

Molar mass	222.7
Average crystal diameter (μm)	~20
Symmetry	Tetragonal
a (Å)	5.3360 (7)
c (Å)	12.457 (2)
V (Å^3)	354.7
Z	4
ρ_{cal}	4.17
Space group	$I4_1/amd$
Radiation	Mo$K\alpha$ (1800 w)
Monochromator	Graphite
Scan mode	θ–2θ
Take off (°)	1.8
Record limits	$\theta < 30°$
Linear absorption coefficient μ (cm^{-1})	87.1
No. of intensities	
Recorded ($\frac{1}{4}$ of Ewald sphere)	327
Unique and nonzero (R_i)[a]	152 (0.015)
Kept[b] ($\sigma(I)/I < 0.30$)	56
F(000)	424
No. of parameters	7
Final R value	0.0345
Final R_w value	0.0363
$w = 0.1635/(\sigma^2(F_0) + g(F_0)^2)$	$g = 0.00665$

[a] Average of the equivalent reflections obtained with the MERG choice of the SHELX program. R_i is the internal consistency factor.

[b] The very small size of the crystal explains the limited number of reflections satisfying the statistical criterion.

atomic distances are given in Table III, as well as the most important angles.

The crystal chemistry of β-$Fe_2(PO_4)O$

TABLE II

β-$Fe_2(PO_4)O$: POSITIONAL AND THERMAL PARAMETERS FROM THE SINGLE CRYSTAL X-RAY STUDY AT 293 K

Atoms	Position	Symmetry	x	y	z	B(Å^2)
Fe	8d	2/m	0	0	$\frac{1}{2}$	0.51(6)
P	4a	42m	0	$\frac{1}{2}$	$\frac{1}{4}$	0.48(14)
O(1)	16h	m	0	0.4950(20)	0.8075(6)	0.49(37)
O(2)	4b	42m	0	$\frac{1}{2}$	$\frac{3}{4}$	0.70(14)

Note. Estimated standard deviation is given in parentheses.

TABLE III

INTERATOMIC DISTANCES (Å) AND ANGLES (°) AT 293 K

Fe–O(1)	(×4)	2.036(7)
O(2)	(×2)	2.0504(2)
Fe–Fe	(×2)	2.6680(3)
	(×4)	3.6411(4)
P–O(1)	(×4)	1.554(9)
O(1)–O(1)	(×2)	2.50(1)
O(1)–O(1)		2.614(2)
O(1)–O(2)		2.649(8)
O(1)–O(1)		2.72(2)
O(1)–P–O(1)	(×4)	107.01
O(1)–P–O(1)	(×2)	114.50
Fe–O(2)–Fe		81.17
Fe–O(2)–Fe		125.22
Fe–O(1)–P		138.81

($NiCrPO_5$-type structure) is discussed in Ref. (*1*), where a projection of the structure can also be found. The most important consequence of the present structure refinement is the confirmation of the space group, because it determines the point symmetries of the different atoms, especially Fe within its octahedron, and, as a consequence, the distribution of electrons among 3d orbitals. This is of importance for our understanding of orbital overlap between nearest neighbor cations and electron transfer between them. The results also confirm that Fe sits on a single crystallographic site.

Magnetism

The susceptibility has been measured from 4 to 850 K with a Faraday balance equipment and a magnetic field of 1.5 T (max). The results are shown in Figs. 2 to 4. An essential point, when comparing these results with our previous measurements (*1*), is that the magnetization, extrapolated at zero field, is in the range of 0.01 emu/g at room temperature, instead of 0.1 emu/g previously. This confirms the improved purity of the present sample (no Fe_3O_4 traces).

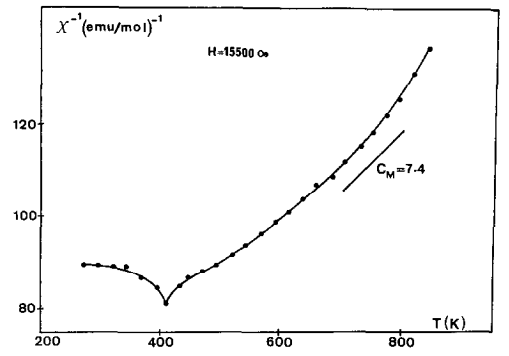

FIG. 2. Reciprocal susceptibility vs temperature.

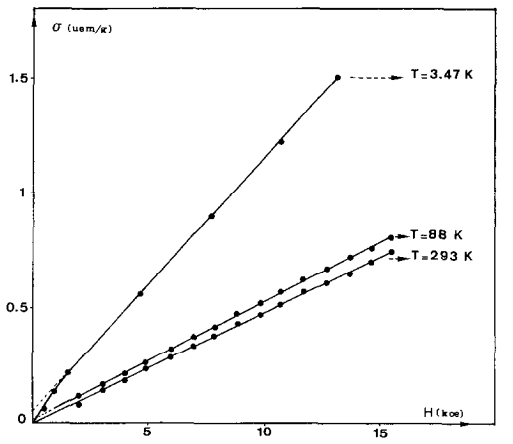

FIG. 3. Magnetization vs applied field at different temperatures.

The high-temperature range, 300–850 K, confirms that there is an antiferromagnetic–paramagnetic transition at T_N = 408 K, and that above this temperature the behavior departs from the Curie–Weiss law. The apparent Curie molar constant C_M would be around 10.5 in the pseudo-linear range from 600 to 750 K, and the expected spin-only value 7.4 is shown on this figure.

At low temperature there is another unusual feature, since the magnetization curve presents a kind of plateau, between 100 K and 300 K, and a small maximum at 12 K.

Magnetic Structure Determination

Low temperature neutron diffraction data were collected on diffractometer D2b at the ILL, Grenoble, France, using the high intensity configuration. The sample was loosely packed into a 16-mm vanadium can and a continuous scan in the range 0–140° 2θ, step size 0.025° 2θ, was performed at 4, 17, and 465 K. A wavelength of 1.5946 Å was used with 150,000 monitor counts per step.

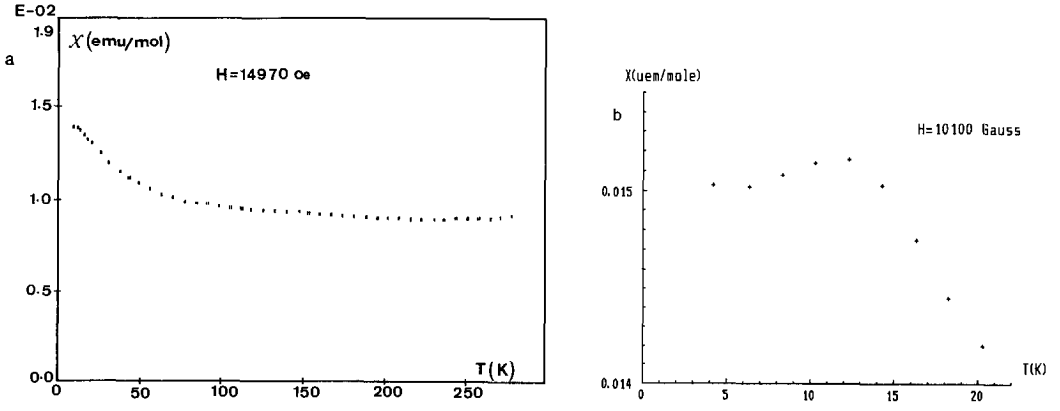

FIG. 4. (a) Susceptibility vs temperature between 10 and 278 K. (b) Susceptibility vs temperature between 4.2 and 20.3 K.

TABLE IV

RESULTS OF THE REFINEMENT OF THE NUCLEAR STRUCTURE OF β-Fe_2PO_5 AT 465 K USING POWDER NEUTRON DATA

Atoms	Position	Symmetry	x	y	z	B(Å^2)
Fe	8*d*	2/*m*	0	0	$\frac{1}{2}$	0.93(4)
P	4*a*	42*m*	0	$\frac{3}{4}$	$\frac{1}{8}$	0.49(6)
O(1)	16*h*	*m*	0	0.4867(3)	0.8080(1)	0.88(4)
O(2)	4*b*	42*m*	0	$\frac{1}{4}$	$\frac{3}{8}$	0.75(6)

Note. R_{WP} = 7.94%, R_P = 6.03%, R_{NUC} = 7.63%, R_{EX} = 2.25%. e.s.d.'s in parentheses.

TABLE VI

CELL PARAMETERS AND VOLUMES (WITH E.S.D.'S IN PARENTHESES) OF β-Fe_2PO_5 AT 17 AND 465 K, REFINED BY USING 7–117° 2θ NEUTRON PROFILES

	4 K	17 K	465 K
a (Å)	5.3500(2)	5.3417(2)	5.3573(2)
c (Å)	12.4791(6)	12.4846(7)	12.5046(5)
c/*a*	2.3325(2)	2.3372(2)	2.3341(2)
Cell volume (Å^3)	357.18(4)	356.23(4)	358.90(4)

Note. The e.s.d.'s take no account of the uncertainty in the neutron wavelength.

Nuclear and magnetic structure refinements were performed by the Rietveld profile technique (*5*). The program PROFPV (Version 1.3) (*6*), a local modification of the Rietveld–Hewat code, was used; the program allows average magnetic intensities to be calculated in a uniaxial configurational spin symmetry. The magnetic form factors used for Fe were from the 3*d* atomic scattering function (spherical part only) determined by Freeman and Watson (*7*).

The nuclear structure was refined in space group $I4_1/amd$ from data collected at 465 K, above the antiferromagnetic transition of T_N = 408 K. The final atomic coordinates and temperature factors are given in Table IV, and the corresponding bond lengths and angles, in Table V. The observed and calculated profiles are shown in Fig. 9. The cell constants were refined for the data at 4, 17, and 465 K, and the results are presented in Table VI; values of *c*/*a* are also given.

TABLE V

INTERATOMIC DISTANCES (Å) AND ANGLES (°) FROM NEUTRON DIFFRACTION STUDY

		17 K	465 K
Fe–O(1)	(×4)	2.062(1)	2.076(1)
O(2)	(×2)	2.0540(1)	2.0584(1)
Fe–Fe	(×2)	2.6709(1)	2.6787(1)
	(×4)	3.6481(2)	3.6552(1)
P–O(1)	(×4)	1.527(2)	1.520(1)
O(1)–O(1)	(×2)	2.465(3)	2.455(2)
O(1)–O(1)		2.549(4)	2.536(3)
O(1)–O(2)		2.674(2)	2.688(1)
O(1)–O(1)		2.793(4)	2.811(5)
O(1)–P–O(1)	(×4)	107.65(5)	107.70(5)
O(1)–P–O(1)	(×2)	113.2(1)	113.1(1)
Fe–O(2)–Fe		81.109(4)	81.184(3)
Fe–O(2)–Fe		125.259(2)	125.214(2)
Fe–O(1)–P		139.25(3)	139.42(3)

The low-angle region of the 465 and 17 K scans is shown in Fig. 5 with the magnetic reflections in the low temperature profile labeled. All of the observed magnetic peaks could be indexed on the tetragonal atomic unit cell with even $h + k + l$ values. This implies that the magnetic cell is body-centered.

Two small peaks, which occur at 11.4° and 14.6° 2θ in lower temperature data, cannot be explained by this model, and may be due to some long range ordering of the Fe (II) and Fe (III). Their appearance as a function of temperature may be seen in Fig. 6 where profiles collected at temperatures from 3.4 to 15.5 K are shown. *c*/*a* also changes between 17 and 4 K (Table VI).

In the nuclear structure, Fe (II/III) occupies one crystallographic site and exists in face-shared FeO_6 octahedra which form continuous chains in the [100] and [010] directions. Two possible antiferromagnetic models were refined; face-shared Fe with opposite spins and face-shared Fe with the

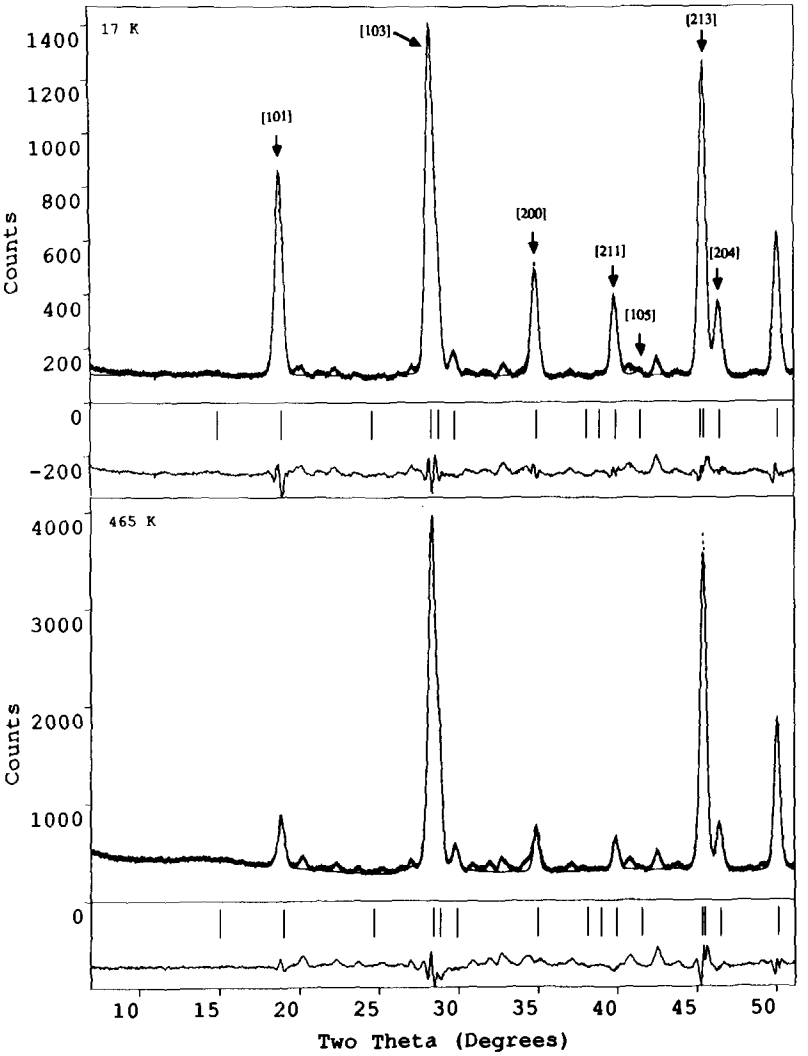

FIG. 5. Low angle regions of the neutron diffraction patterns at 17 and 465 K with magnetic peaks labeled (λ = 1.5946 Å).

same spin direction along each chain, but chains in the [100] direction having spin up and those in the [010] direction having spin down. These models are illustrated in Fig. 7.

We first considered the antiparallel face-sharing Fe model, (Fig. 7a), and an examination of the magnetic peak intensities and indices indicated spin in the [001] direction. Refinement of this model confirmed that the spin was primarily in the [001] direction, but the profile fit was considered inadequate for the model in Fig. 7a to be correct. The second model (Fig. 7b), with parallel spins in each chain of FeO_6 octahedra, but chains running in the [010] direction having spin up and those in the [100] direction having spin down, was refined and gave much better R-factors. In view of the weak ferromagnetism detected in the magnetic sus-

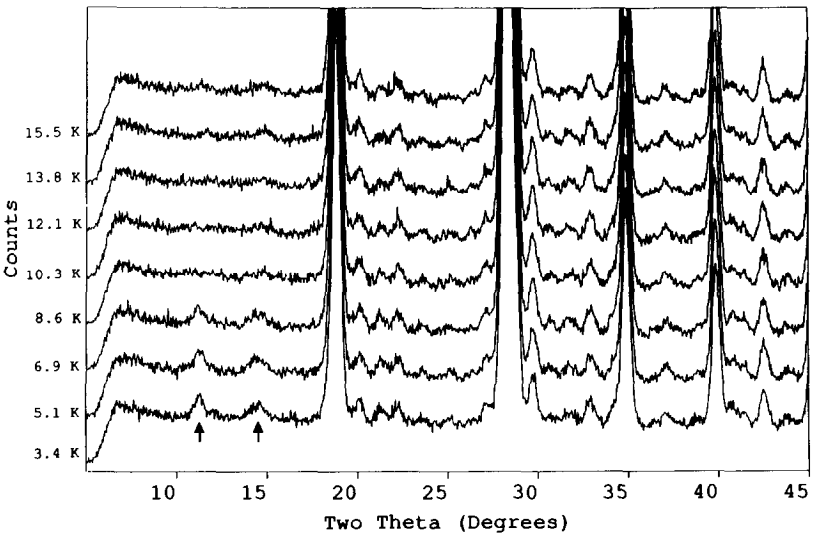

FIG. 6. Low angle regions of the neutron diffraction patterns collected at 3.4, 5.1, 6.9, 8.6, 10.3, 12.1, 13.8, and 15.5 K.

ceptibility work at low temperatures, a third model was tried, based on the second, but allowing for a weak ferromagnetic component in the *xy* plane. This did not prove to be as stable or fit as well as the antiferromagnetic model and was rejected. The final magnetic model is illustrated in Fig. 8.

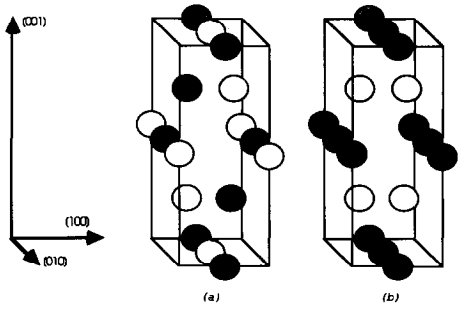

FIG. 7. Diagrammatic representation of the possible spin arrangements on the Fe face-shared octahedral sites. The shading indicates opposite spin direction. In (a) each chain of FeO_6 octahedra is ordered antiferromagnetically, whereas in (b) the Fe within each chain are ordered ferromagnetically, but the magnetic ions in chains running in the [100] direction are of opposite spin to those in the [010] direction.

Profile data above 126° 2θ were excluded due to excessive peak broadening; as no peaks were detected below 7° 2θ, this region was also excluded to reduce errors from noise at low angles. The *R*-profile is higher than expected because of extra peaks due to the presence of impurities within the sample (the neutron diffraction has been carried out on a batch prepared from $(NH_4)_2HPO_4$ and not by the new method described above). These regions were not excluded because the number of extra peaks is large although their relative

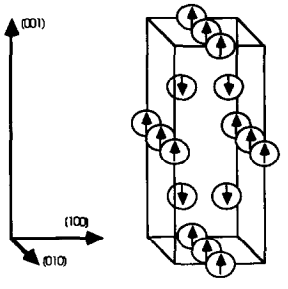

FIG. 8. Refined magnetic structure of β-Fe_2PO_5 showing the spin directions on the Fe sites.

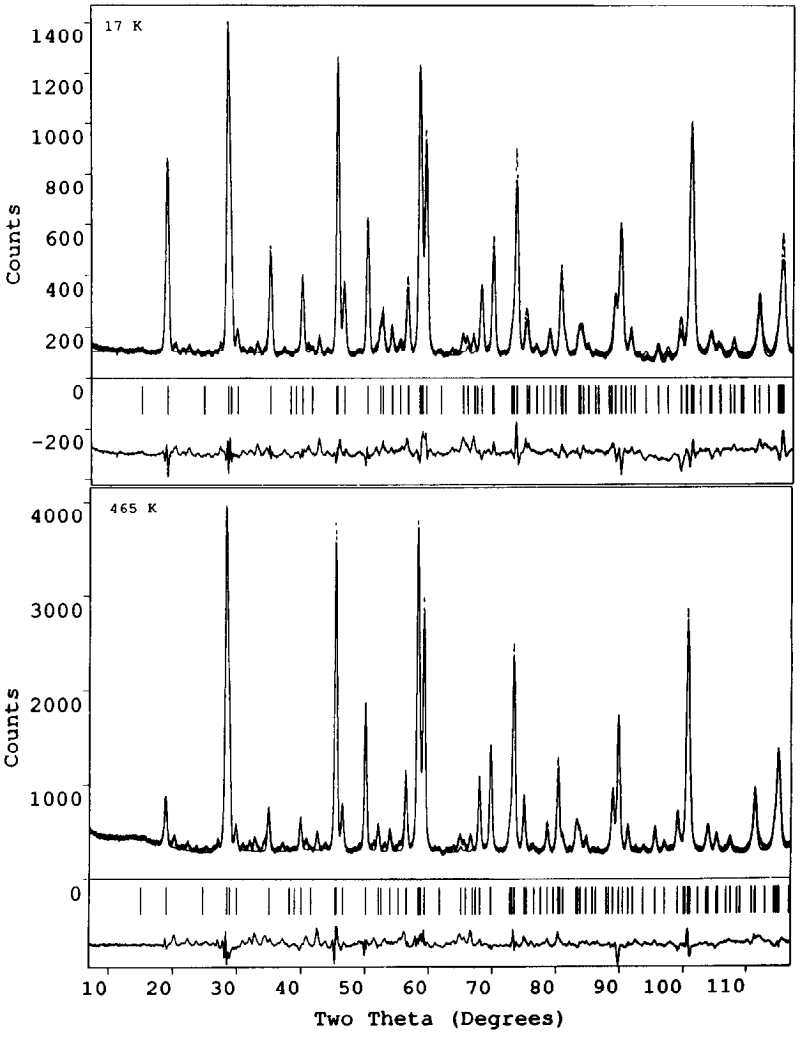

FIG. 9. Observed and calculated neutron powder diffraction profiles of β-Fe_2PO_5 at 17 and 465 K.

intensity is quite low. The final refinement is shown in Fig. 9. The results of the 17 K refinement are given in Table VII, and bond distances and angles are given in Table V.

Discussion

β-$Fe_2(PO_4)O$ presents several peculiarities:

Above T_N, the apparent Curie constant shifts progressively from an abnormally

TABLE VII

RESULTS OF THE REFINEMENT OF THE NUCLEAR AND MAGNETIC STRUCTURE OF β-Fe_2PO_5 AT 17 K USING POWDER NEUTRON DATA

Atoms	Position	Symmetry	x	y	z	B(Å^2)
Fe	8*d*	2/*m*	0	0	$\frac{1}{2}$	0.11(4)
P	4*a*	42*m*	0	$\frac{1}{4}$	$\frac{1}{8}$	0.11(4)
O(1)	16*h*	*m*	0	0.4886(3)	0.8077(1)	0.46(4)
O(2)	4*b*	42*m*	0	$\frac{1}{4}$	$\frac{3}{8}$	0.93(7)

Note. Magnetic component of Fe, $\mu_z = 4.17(3)\ \mu_B$. $R_{WP} = 10.24\%$, $R_P = 7.39\%$, $R_{NUC} = 7.71\%$, $R_{MAG} = 9.89\%$, $R_{EX} = 3.10\%$. e.s.d.'s in parentheses.

high value toward an abnormally low one. This may indicate that the magnetic order is not completely destroyed above T_N (short-range interactions), yielding a high apparent Curie constant. As the temperature increases, electron delocalization takes place at a high frequency (we have previously (*1*) shown that the relaxation frequency reaches $\sim 10^8$ Hz at ~500 K), and the usual calculation fails. We also note that, just above T_N, the χ^{-1} vs T curvature corresponds to a ferromagnetic tendency, which is consistent with the neutron results.

Below T_N, the small maximum of χ at 12 K remains unexplained and might be related to a transition of the Verwey type at 120 K in magnetite, that is an order–disorder transition of the minority spin electrons. This could introduce a small distortion below the transition, as shown by the two additional lines detected in the neutron diffraction diagram below 10 K.

In this respect, the following additional observations are of interest:

(i) A small ferromagnetic component (~0.055 emu/g) is observed at 4 K, as shown in Fig. 3.

(ii) The Mössbauer spectra at 4 and 20 K do not display any difference.

(iii) Investigation of a possible spin glass at low temperature, through temperature cycles at 500, 1000, and 2000 Oe, did not bring any indication of such a magnetic state.

(iv) As possible impurities, we have especially looked for $Fe_3(PO_4)_2$, $Fe_7(PO_4)_6$, $FePO_4$, and of course Fe_3O_4. However, the Néel temperatures are respectively, 44 K (*9*) and less than 10 K (*10*), for the two first phosphates; $FePO_4$ would be easily detected because of its strong diffraction line at 3.45 Å; Fe_3O_4 does not display any singularity at 12 K, and moreover it would contribute a ferromagnetic component (0.055 emu/g correspond to 0.05% Fe_3O_4 only).

On the whole, there are some indications for a transition at 12 K: additional diffraction lines, a change in c/a between 17 K and 4 K, and a small ferromagnetic component at low temperature. However, the exact nature of this transition remains to be investigated.

The arrangement of parallel spins between the face-sharing FeO_6 octahedra is not a surprising result. Double exchange interactions are observed for the Fe(II) and Fe(III) in octahedral sites in Fe_3O_4 (*8*). The easiest electron to transfer from the high-spin Fe(II) to a neighboring Fe(III) is the minority spin electron, since this mechanism sustains the maximum exchange energy. Such a transfer is only possible if the two ions are aligned ferromagnetically. However the antiferromagnetic interaction is also strong (for instance in Fe_3O_4, $J_{AB} \simeq -2.3$ meV and $J_{BB} \simeq 0.68$ meV according to Ref. (*11*)), and contributes to the same spin arrangement. Moreover, the 90° exchange via oxygen between the face-sharing Fe(II)/Fe(III) is also ferromagnetic (roughly equivalent to J_{BB} in Fe_3O_4). This is why the Néel temperature is rather high and the short-range magnetic order persists above T_N.

References

1. B. Ech-Chahed, F. Jeannot, B. Malaman, and C. Gleitzer, *J. Solid State Chem.* **74,** 47 (1988).
2. C. Gleitzer and J. B. Goodenough, *Struct. Bond.* **61,** 1 (1985).
3. J. A. Ibers and W. C. Hamilton (Eds.), "International Tables for X-ray Crystallography," Vol. 4, Kynoch Press, Birmingham (1974).
4. G. M. Sheldrick, "Shelx 76—Program for Crystal Structure Determination," University of Cambridge, England (1976).
5. H. M. Rietveld, *J. Appl. Crystallogr.* **2,** 65 (1969).
6. B. Toby, D. E. Cox, and P. Zollicker, personal communication (1989).

7. A. J. FREEMAN AND R. E. WATSON, *Acta Crystallogr.* **14,** 231 (1961).
8. P. A. COX, "The Electronic Structure and Chemistry of Solids," Oxford Univ. Press, London/New York (1987).
9. T. ERICSSON AND A. G. NORD, *Amer. Mineral.* **69,** 889 (1984).
10. G. J. LONG, A. K. CHEETHAM, AND P. D. BATTLE, *Inorg. Chem.* **22,** 3012 (1983).
11. D. H. TORRIE, *Solid State Commun.* **5,** 715 (1967).
12. C. N. R. RAO AND K. J. RAO, "Phase Transitions in Solids," McGraw–Hill, New York (1978).